Carbohydrate Polymers 85 (2011) 376–387

Contents lists available at ScienceDirect

Carbohydrate Polymers

journal homepage: www.elsevier.com/locate/carbpol

Adsorption of cefotaxime sodium salt on polymer coated ion exchange resin microparticles: Kinetics, equilibrium and thermodynamic studies

S. Vasiliu*, I. Bunia, S. Racovita, V. Neagu

"Petru Poni" Institute of Macromolecular Chemistry, Gr. Ghica Voda Alley No. 41A, 700487 Iasi, Romania

ARTICLE INFO

Article history:
Received 23 July 2010
Received in revised form 15 February 2011
Accepted 22 February 2011
Available online 1 March 2011

Keywords:
Ion exchange resin
Polysaccharide
Adsorption isotherm
Adsorption kinetics
Thermodynamic studies

ABSTRACT

Microparticles with complex architectures based on the polyelectrolyte complexes between an acrylic ion exchange resin and two polysaccharides: gellan and xanthan gum were prepared and used for the adsorption of antibiotic in order to obtain a new drug delivery systems. Batch adsorption studies have been carried out to determine the effect of the contact time, temperature and the initial concentration of drug solution on the adsorption behavior. The Langmuir, Freundlich, Temkin and Dubinin–Radushkevich adsorption isotherms were used to model this behavior. The kinetics were fitted with the pseudo-first order, pseudo-second order, Elovich and intraparticle diffusion models. The best results were achieved with pseudo-second order kinetic model. The thermodynamic parameters (ΔG, ΔH, ΔS) were also calculated and the values indicate that the adsorption process was endothermic and spontaneous. The results showed that the microparticles with complex structures have a higher adsorption capacity, making it suitable for use in drug delivery systems.

1. Introduction

The idea of controlled drug delivery has been known since the 1930, but the modern history of drug delivery begins in 1968 when the Alza Company released a new concept of "therapeutic system" by introducing pharmaceutical formulations that would help to stabilize the amount of drug in the patient's bloodstream. In controlling drug delivery systems, an active therapeutic agent is immobilized into a polymeric network structure in such a way that the drug is released from the macromolecular support in a predefined manner.

In modern medicine, natural and synthetic polymeric materials with various architectures have been developed to achieve two main objectives: (1) to optimize the drug therapeutics and (2) to improve patient compliance. A combination between synthetic and natural polymers could lead to new polymeric materials with specific properties for delivery of low and high molecular weight drugs.

Among the synthetic polymers, the ion exchange resins have received considerable attention since the 1930. Initially ion exchange resins were developed for industrial and agricultural applications, such as waste water purification (Dulman, Simion, Barsanescu, Bunia, & Neagu, 2009; Neagu, Untea, Tudorache, & Orbeci, 2004) and separation of different gases. More recently they have been used in pharmaceutical and medical fields for isolation and purification of pharmaceutical active ingredients (Belakhov & Momot, 1983) or as functional excipients in dosage form (taste masking agent, tablet disintegrant, drug stabilization agent and sustained release agent) and or active drug ingredients. From a therapeutic standpoint it is well known that colestipol (a weakly basic ion exchange resin), cholestyramine (a strongly basic ion exchange resin) and colesevelam act as cholesterol reducers (Angelin & Einarsson, 1981), Kayexalate (sodium polystyrene sulfonate) is approved for use in the treatment of hyperkalemia (Sterns, Rojas, Bernstein, & Chennupati, 2010), sevelamer (weakly basic anion exchange resin in the chloride form) is used for the management of hyperphosphataemia in chronic renal failure (Wrong & Harland, 2007) and nicorette gum, a product based on anionic exchange resin is used in smoking cessation programs (Conaghey, Corish, & Corrigan, 1998).

Also, the ion exchange resin can be used as site-specific drug delivery systems, such as gastric retentive systems, sigmoidal release systems, site-specific delivery of anti-cancer drugs, ophthalmic drug delivery, nasal drug delivery and iontophoretically assisted transdermal system (Atyabi, Sharma, Mohammad, & Fell, 1996; Holmberg et al., 1999).

Their high capacity of drug loading, the presence of the functional groups, the controlled or sustained release of drug, reduction of the degradation of drug molecules in the gastrointestinal tract, physico-chemical stability, their insolubility in any solvents are several properties of ion exchange resins that highlight their ability to be an ideal candidates for use as sustained release systems of bioactive compounds. Because in the presence of an excess of ions the drug release from the matrix can be very fast, a polymeric

* Corresponding author. Tel.: +40 232 217454; fax: +40 232 211299.
E-mail address: msilvia@icmpp.ro (S. Vasiliu).

0144-8617/$ – see front matter © 2011 Elsevier Ltd. All rights reserved.
doi:10.1016/j.carbpol.2011.02.039

Table 1
Physicochemical characteristic of started acrylic resin and of drug.

Physicochemical properties of started acrylic ion exchange resin		
Type	Weakly base	
Matrix	Ethyl acrylate, acrylonitrile and divinylbenzene copolymer functionalized with ethylene diamine	
Functional group	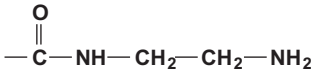	
Ionic form used in this study	Chloride	
Crosslinking	3%	
Exchange capacity	0.31 meq./mL or 7.47 meq./g	
Diameter size	300–800 μm	
Physicochemical properties of CF		**Ref.**
Molecular structure	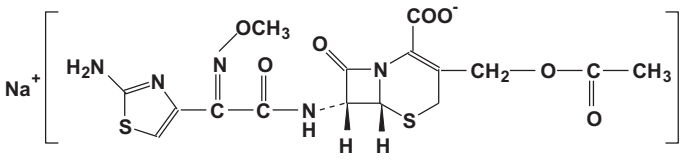	
Molecular formula	$C_{16}H_{16}N_5NaO_7S_2$	
Molecular weight	477.4 g/mol	
Solubility	H_2O: 50 mg/mL poorly soluble in common organic solvents including ethanol	
pK_a	pK_{a1} = 2.1 pK_{a2} = 3.4 pK_{a3} = 10.9	[19]
Physical form	Crystalline powder	
Color	White to yellow	
Stability	Aqueous solution of pH = 4.3–6.2 are stable up to 3 weeks at 2–8 °C	
UV–vis wavelength	λ = 236 nm	

film or waxy layer can be applied onto the surface of drug–ion resin complex (Jeong, Berhane, Haghighi, & Park, 2007).

The knowledge about the factors that determine the interaction between the drug and macromolecular support is relevant in the design of pharmaceutical dosage forms. In literature, there have been many studies on the drug release from drug-resinate products (Albertini et al., 2008; Fundueanu et al., 2005) while less work has been conducted on the adsorption kinetics, equilibrium and thermodynamic studies of drug onto different adsorbents (Abdekhodaie & Wu, 2006).

In this study, the cefotaxime sodium salt (CF) was used as bioactive compound. Cefotaxime sodium salt is a semi-synthetic broad spectrum cephalosporin indicated for the treatment of patients with serious infections caused by susceptible strains of the designated microorganisms in the various diseases, such as lower respiratory tract infections, genitourinary infections, septicemia, skin infections, intra-abdominal infections including peritonitis, bone and joint infections and central nervous system infections (Connors, Amidon, & Stella, 1986). This antibiotic is especially used for parenteral administration. For patient compliance we tried to find a suitable delivery system for its oral administration.

Initially, the overall objective of this work is to present comparative data on the CF adsorption properties onto an acrylic ion exchange resin and microparticles obtained by coating of its surface with two anionic polysaccharides produced by *Pseudomonas elodea* and *Xanthomonas campestris*, called gellan (Gll) and xanthan gum (Xan). In the future we shall continue to explore the mechanism of drug release from this new drug delivery systems.

2. Experimental

2.1. Materials

Gellan gum and xanthan gum were purchased from Fluka Chemical Company and were used as received.

Acrylic ion exchange resin in the bead form was prepared by suspension polymerization technique, described elsewhere (Bunia, Neagu, & Luca, 2006).

Cefotaxime sodium salt was purchased from Fluka Chemical Company (Connors et al., 1986).

The physicochemical characteristics of acrylic resin and cefotaxime sodium salt are presented in Table 1.

2.2. Methods

2.2.1. Preparation of acrylic ion exchange resin

The acrylic copolymers were synthesized by aqueous suspension copolymerization of divinylbenzene (DVB, 3 wt.%), acrylonitrile (AN, 20 wt.%) and etylacrylate (EA, 77 wt.%) using 1 wt.% of benzoyl peroxide as initiator. To obtain a porous copolymer the copolymerization reaction was carried out in the presence of toluene as a diluent using a dilution, D of 0.4. D = mL toluene/(mL toluene + mL monomers). The aqueous phase consisted of 0.5 wt.% ammonium salt of poly(styrene-co-maleic anhydride) as polymeric stabilizer. The organic/aqueous phase ratio was 1:3. The copolymerization reaction was allowed to proceed for 4 h at 65 °C, 6 h at 75 °C and 4 h at 85 °C. After copolymerization, the copolymers were separated and extracted with dichloroethane in a Soxhlet apparatus to remove traces of residual monomers, linear oligomers and diluent. The content of DVB units in the copolymers was assumed to be the same as the monomer content in feed. Aminolysis reactions were performed at 110–115 °C with ethylenediamine (EDA) under reflux for 14 h in a glass round bottomed flask equipped with stirrer, reflux condenser and thermometer. The copolymer:amine ratio was 1:3. After the reaction, the resin was separated by filtration, washed with water and then regenerated with 4% NaOH aqueous solution. To convert the resin in Cl^- form, resin sample was equilibrated with 1 N HCl for 24 h and then washed with deionized water to remove HCl in excess.

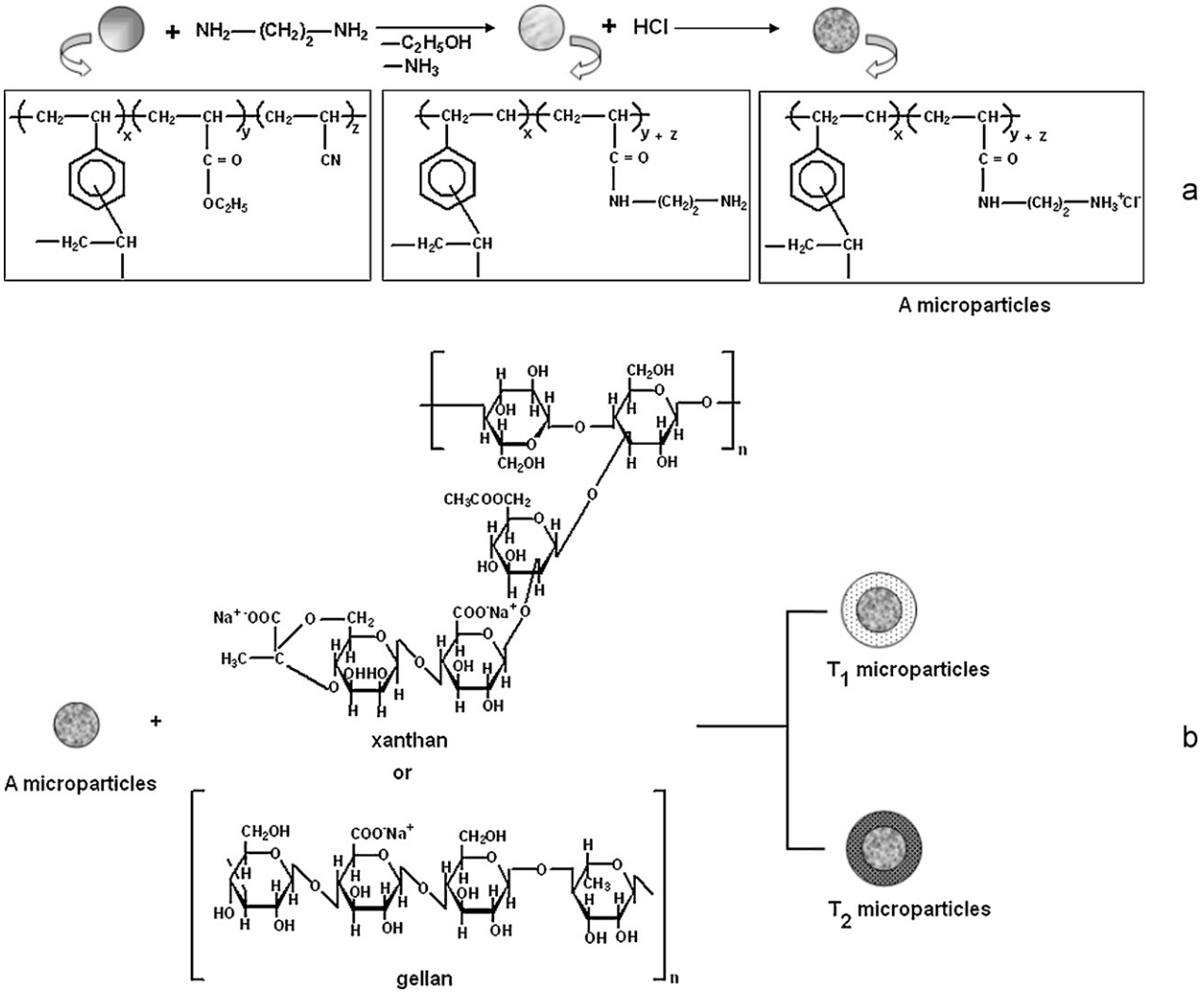

Scheme 1. Schematic representation of preparation method of A microparticles (a) and T microparticles (b).

2.2.2. Preparation of T_1 and T_2 microparticles

5 g of the acrylic ion exchange resin in Cl^- form (A microparticles) were placed in 500 mL of 1% xanthan solution (T_1 microparticles) or 1% gellan solution (T_2 microparticles) at pH = 5.5 and 25 °C for 24 h under a permanent gentle stirring. After the specified time period, the beads were removed from the polysaccharide solutions by filtration, rinsed with distilled water and then centrifuged at 1000 rpm for 10 min. The amount of gellan or xanthan gum interacted with acrylic resin was determined by the following equation:

$$\%\text{Gll or Xan} = \frac{m_i - m_0}{m_0} \times 100 \quad (1)$$

where m_i is the mass of T_1 or T_2 microparticles and m_0 is the mass of A microparticles.

For characterization in the dried state, the microparticles were dried at room temperature for 24 h and under vacuum at 40 °C for 48 h.

2.2.3. Characterization of A, T_1 and T_2 microparticles

T_1 and T_2 microparticles were characterized by FT IR spectroscopy using a Bruker Vertex FT IR spectrometer, resolution 2 cm^{-1} in the range of 4000–400 cm^{-1} by KBr pellet technique.

The surface morphology of the A, T_1 and T_2 microparticles was observed with an Environmental Scanning Electron Microscope type Quanta 200 at 25 kV.

TGA measurements were performed under nitrogen atmosphere at a heating rate of 10 °C/min with a Mettler Toledo model TGA/SDTA 851. The initial mass of sample was 3–5 mg and the weight loss versus temperature was recorded.

2.2.4. Batch adsorption studies

The adsorption of CF on A, T_1 and T_2 microparticles was investigated in a batch system. These experiments can provide information on the contact time required to achieve the optimum condition for adsorbate retention. Batch adsorption experiments were carried out by adding a know amount of A, T_1 and T_2 microparticles (0.5 g) to a set of 100 mL conical flasks filled with 20 mL CF solution with various initial concentrations (70–3750 mg/L). The conical flasks were placed in a thermostated shaker bath (Memmert M00/M01, Germany) and shaken at 180 rpm and 25, 35 and 40 °C for different contact time ranging between 10 min and 24 h until equilibrium was reached. The flasks were than removed from the shaker and the samples were centrifuged at 1000 rpm for 10 min. The concentrations of CF in the supernatant solution before and after adsorption were determined using a UV-VIS Spectrophotometer (UV-VIS SPEKOL 1300, Analytik Jena) at a wavelength of 236 nm.

The amounts of CF at equilibrium, q_e (mg/g) and at any time, q_t (mg/g) were calculated from the following equations:

$$q_e = \frac{(C_0 - C_e) \cdot V}{W} \quad (2)$$

$$q_t = \frac{(C_0 - C_t) \cdot V}{W} \quad (3)$$

where C_0 is the initial concentration of CF solution (mg/L), C_t is the concentration of CF solution at any time (mg/L), C_e is the concentration of CF solution at equilibrium (mg/L), V is the volume of drug solution (L) and W is the amount of microparticles (g). All the adsorption data were achieved in triplicate and the average values were plotted.

3. Results and discussion

3.1. Preparation of T_1 and T_2 microparticles

The T_1 and T_2 microparticles have been obtained by two steps:

(a) synthesis of the crosslinked functional acrylic copolymers (acrylic ion exchange resin) by aminolysis with ethylene diamine of ethylacrylate–divinylbenzene–acrylonitrile copolymer in the bead form (A microparticles);
(b) synthesis of polymer coated ion exchange resin microparticles by interaction between acrylic resin in chloride form and xanthan and gellan gum (T_1 and T_2 microparticles).

The schematic representation of the preparation method of T_1 and T_2 microparticles is presented in Scheme 1.

The percentage of Xan and Gll in the T_1 and T_2 microparticles was determined gravimetrically (Eq. (1)) and was found to be 84% for T_1 microparticles and 81% for T_2 microparticles.

3.2. Characterization of microparticles

3.2.1. FT IR spectra

The FT IR spectroscopy method was used to obtain information on the nature of possible interactions between the functional groups of the acrylic resin and two polysaccharides. The FT IR spectra of A, T_1 microparticles as well as of Xan were presented in Fig. 1.

As could be seen from the FT IR spectrum of xanthan (Fig. 1, Xan) a board band at 3435 cm^{-1} is attributed to –OH stretching vibration. The band at 2918 cm^{-1} represents the >CH– stretching vibrations belonging to $>CH_2$ group and the band at 1734 cm^{-1} indicates the >C=O stretching of acetyl group. The adsorption bands at 1622 and 1408 cm^{-1} correspond to the asymmetric and symmetric stretching vibration of carboxylate anions from pyruvate and glucuronate groups.

For the acrylic exchange resin the following characteristic absorption bands are observed: the band at 3081 cm^{-1} corresponds to the asymmetric stretching vibration of the ring C–H bonds or $–NH_3^+$ groups; the band at 1656 cm^{-1} indicates the presence of the amide groups; the ring carbon–carbon stretching and the asymmetric stretching vibration of $>CH_2$ groups appear at 1448 cm^{-1} as well as at 1389 cm^{-1}.

The spectrum of T_1 microparticles exhibits some differences such as: (1) the presence of two absorption bands at 1654 and 1649 cm^{-1} belonging to the both polymers; (2) appearance of the absorption band at 1294 cm^{-1} which corresponds to the –OH groups from xanthan; (3) the NH_3^+ band from A microparticles spectrum at 1557 cm^{-1} shifted to the higher frequency (1560 cm^{-1}) indicating an active participation of these groups in the formation of ionic bonds with carboxylate groups of xanthan.

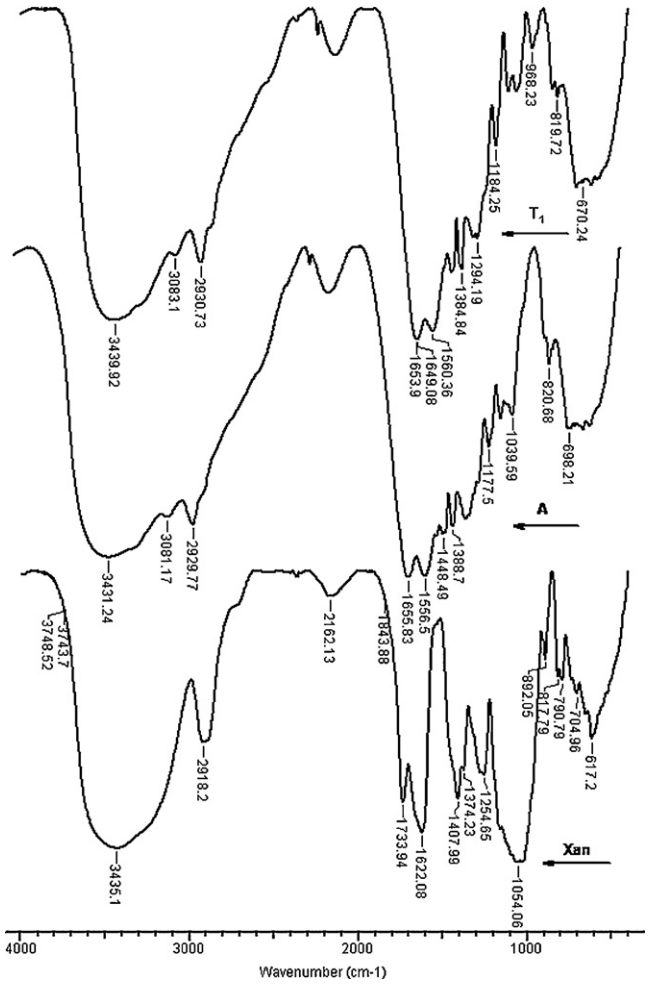

Fig. 1. FT-IR spectra of xanthan, A and T1 microparticles.

Based on the above observations, it can be asserted that T_1 microparticles are formed by ionic interactions, without excluding the possibility of other type of interactions between the two polymers, i.e. hydrogen bonds.

3.2.2. SEM microscopy

A, T_1 and T_2 microparticles have showed a good sphericity with an average diameter size ranging between 300 and 800 μm. For the adsorption studies the fractions with diameter size ranging between 300 and 500 μm were taken into consideration. SEM images of acrylic ion exchange resin before and after reaction with polysaccharides are shown in Fig. 2a–d.

Fig. 2d shows a visible change of the surface morphology of T microparticles compared with A microparticles (Fig. 2b) demonstrating the formation of the interpolymer complex between the acrylic resin and polysaccharides.

3.2.3. Thermogravimetric analysis

The thermogravimetric analysis data and the TGA thermograms of Gll, Xan, A, T_1 and T_2 are shown in Table 2 and Fig. 3, respectively.

The thermogravimetric analysis of acrylic resin (Bunia et al., 2006), gellan and xanthan is well known in literature (Ciardelli et al., 2005; Sand, Yadav, & Behari, 2010). The temperature at which intensive degradation is initiated (T_i) was viewed as a criterion of heat stability of the new materials. As shown in Table 2, the main decomposition regions for Xan and Gll start at 210 °C and 190 °C and end at 335 °C and 315 °C with weight losses of 49% and 51.5%, respectively. For acrylic resin the decomposition stage starts

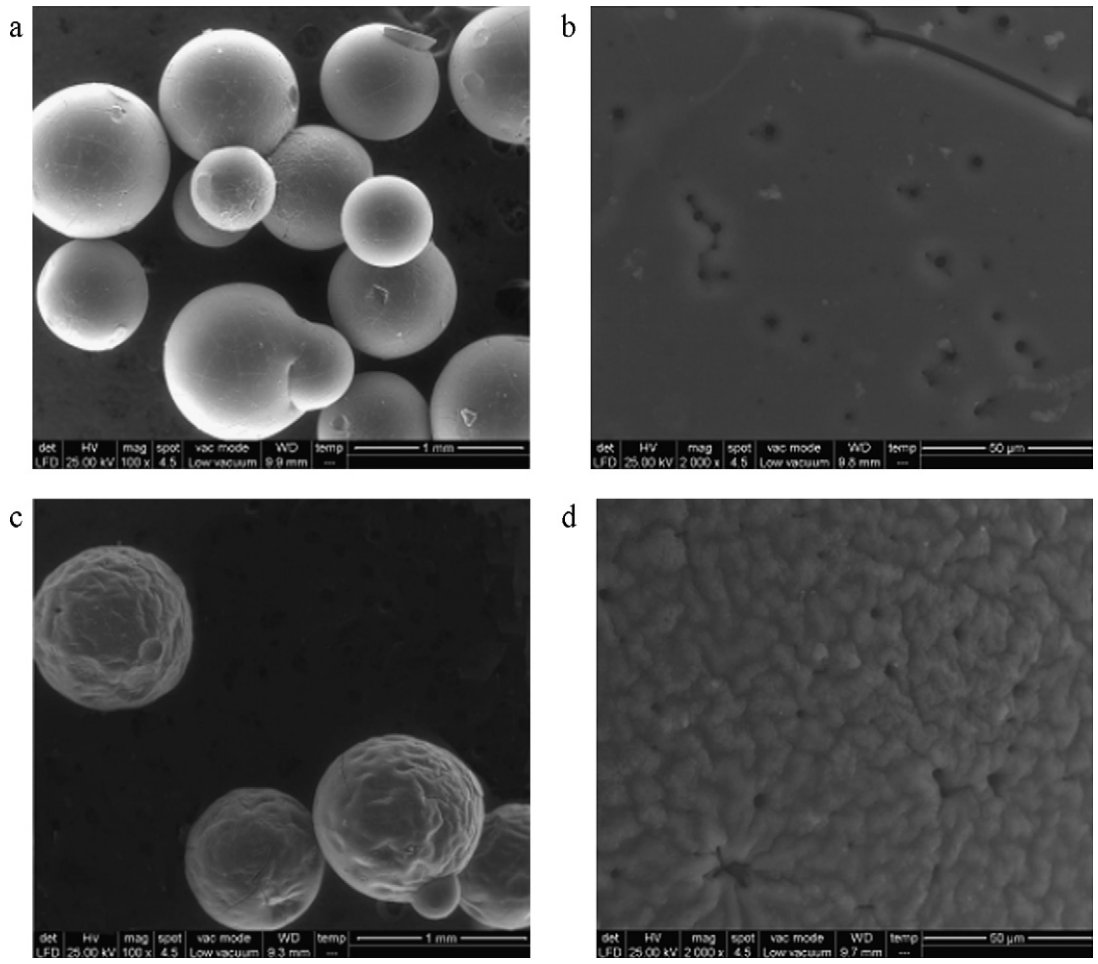

Fig. 2. SEM images for A (a and b) and T_1 microparticles (c and d).

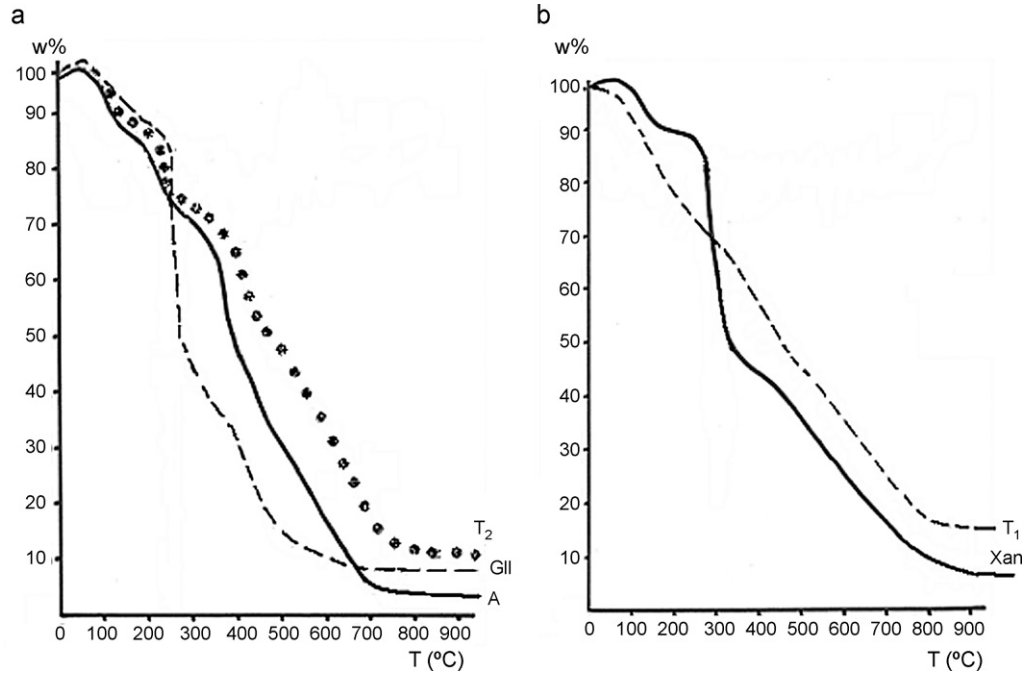

Fig. 3. TGA thermograms for: Gll, A and T_2 microparticles (a) and Xan and T_1 microparticles (b).

Table 2
Thermogravimetric characteristics of main degradation stage for Gll, Xan, A, T_1 and T_2 microparticles.

Sample code	Decomposition temperature (°C)[a]			Weight loss
	(%)	T_{max}	T_f	
Gll	190	235	315	51.5
Xan	210	270	335	49
A	260	330	430	39
T_1	285	380	465	22
T_2	270	355	450	26

[a] T_i: initial degradation temperature; T_{max}: temperature of maximum rate of weight loss; T_f: finally degradation temperature.

at 260 °C and ends at 430 °C with weight losses of 39%. T_1 and T_2 microparticles are found to have higher thermal stability than starting polymers because the decomposition stages start at 285 °C and 270 °C and end at 465 °C and 450 °C with weight losses of 22% and 26%, respectively. These results confirm the formation of the interpolymer complexes between the functional groups belonging to the acrylic resin and Xan or Gll.

3.3. Adsorption studies

In order to evaluate the adsorption process, it requires under consideration of two important physico-chemical aspects as follows: the equilibrium and the kinetics of adsorption.

3.3.1. Equilibrium isotherm

The adsorption isotherms can give the most important information about the distribution of the adsorbate molecules between the liquid and solid phases when the adsorption process reaches an equilibrium state. Various isotherm equations like those Langmuir, Freundlich, Temkin and Dubinin–Radushkevich were used to describe the equilibrium characteristics of adsorption.

3.3.1.1. Langmuir isotherm. In 1918, Langmuir has developed a theoretical equilibrium isotherm relating to the amount of gas adsorbed on a surface. Now, this model is a well-known isotherm model and widely used to quantify the performance of different adsorbents (Chen & Huang, 2010; Wawrzkiewicz & Hubicki, 2010). The Langmuir equation is applicable to homogeneous adsorption based on the following assumptions:

(1) adsorption can only occur at a finite number of definite localized sites;
(2) all binding sites posses the same affinities for adsorption of a single molecular layer;
(3) there is no transmigration of the adsorbate on the plane of the surface;
(4) all sites are of equal size and shape on the surface of adsorbent.

The Langmuir equation is given as:

$$\frac{C_e}{q_e} = \frac{1}{q_m \cdot K_L} + \frac{C_e}{q_m} \quad (4)$$

where q_m is the maximum adsorption capacity (mg/g), K_L is the Langmuir constant (L/mg) related to the energy of adsorption which reflects the affinity between the adsorbent and adsorbate.

A plot C_e/q_e versus C_e (figure not shown) yields a straight line with slope $1/q_m$ and intercepts $1/q_m \cdot K_L$. The values of Langmuir equation parameters are given in Table 3.

The monolayer saturation capacities (q_m) at 313 K are 962.07 mg/g for A microparticles, 1029.46 mg/g for T_1 microparticles and 980.39 mg/g for T_2 microparticles. The q_m values for CF obtained from Langmuir model are much higher than the highest adsorption capacities resulted by the batch adsorption experiments (Tables 4–7). Also, from Table 3 it is observed an increase of the saturation capacity with increase of temperature which reflects a better accessibility of the sorption sites. Based on K_L value T_1 microparticles show a higher affinity for CF, which is well correlated with the higher adsorption capacity obtained for T_1 microparticles. The essential characteristics and the feasibility of the Langmuir model were expressed by Weber and Chakravot (1974) in terms of a dimensionless constant, commonly known as separation factor (R_L) which is expressed by the following equation:

$$R_L = \frac{1}{1 + K_L \cdot C_0} \quad (5)$$

The R_L values indicate either the shape of adsorption isotherm is unfavorable ($R_L > 1$) or favorable ($0 < R_L < 1$) or linear ($R_L = 1$) or irreversible ($R_L = 0$).

Values of R_L calculated at 25, 35 and 40 °C for all concentrations of drug solutions (Table 3) were in range between 0 and 1, which indicate that the adsorption process is favorable at operation conditions studied. For each type of microparticles the R_L value decreases with the rise of temperature, suggesting an increase of the affinity between CF and microparticles. Since the results obtained on the adsorption of CF on A, T_1 and T_2 microparticles do not fit well with Langmuir model an attempt was made to fit the experimental data to the Freundlich model.

Table 3
Langmuir, Freundlich, Dubinin–Radushkevich and Temkin parameters for the adsorption of CF on A, T_1 and T_2 microparticles at different temperatures.

T (°C)	A			T_1			T_2		
	298	308	313	298	308	313	298	308	313
Langmuir									
q_m (mg/g)	877.19	952.38	962.07	813.01	934.58	1029.46	884.96	952.38	980.39
K_L ($\times 10^2$ L/mg)	4.65	5.93	6.39	11.86	13.26	13.86	8.23	9.65	10.30
R_L	0.235	0.194	0.182	0.107	0.097	0.093	0.147	0.129	0.122
R^2	0.984	0.986	0.988	0.990	0.990	0.978	0.987	0.978	0.959
Freundlich									
K_F (L/g)	2.002	3.654	7.433	7.416	10.44	11.89	5.04	8.73	9.87
$1/n$	0.703	0.649	0.568	0.582	0.551	0.549	0.619	0.577	0.554
R^2	0.997	0.999	0.999	0.995	0.998	0.998	0.995	0.999	0.999
Dubinin–Radushkevich									
q_m (mg/g)	453.95	530.75	556.70	604.40	657.63	728.83	548.35	601.74	678.69
E (kJ/mol)	2.59	5.34	7.05	4.95	6.95	7.94	3.70	6.04	7.68
R^2	0.999	0.991	0.991	0.998	0.998	0.997	0.997	0.994	0.995
Temkin									
b_T (J/mol)	13.99	13.83	13.61	12.51	12.49	11.66	12.71	12.57	12.48
a_T (L/mg)	0.0056	0.0069	0.0099	0.0107	0.0135	0.0146	0.0083	0.0127	0.0132
R^2	0.988	0.989	0.991	0.998	0.996	0.995	0.995	0.985	0.985

Table 4
Kinetic parameters and their correlation coefficients for the adsorption of CF onto A, T_1 and T_2 microparticles (C_{CF} = 70 mg/L).

Sample code	A			T_1			T^2		
Temperature (K)	298	308	313	298	308	313	298	308	313
$q_{e,exp}$ (mg/g)	9.92	14.98	17.27	15.30	17.65	19.25	12.92	15.30	17.88
The Lagergren's pseudo first order model									
q_e (mg/g)	8.43	10.60	12.66	8.38	8.66	8.88	7.51	8.03	9.20
k_1 ($\times 10^3$ min^{-1})	4.42	3.75	5.37	4.74	4.24	4.68	5.78	4.54	3.96
R^2	0.987	0.988	0.985	0.975	0.979	0.980	0.977	0.983	0.980
Ho pseudo-second order model									
q_e (mg/g)	10.89	15.83	18.25	15.82	18.05	19.62	13.34	15.67	18.18
k_2 ($\times 10^4$ g/(mg min))	7.73	7.86	8.29	18.8	19.3	20.26	16.9	17.6	18.5
h (mg/(g min))	0.0917	0.197	0.276	0.47	0.63	0.78	0.30	0.43	0.61
R^2	0.999	0.999	0.999	0.999	0.999	0.999	0.999	0.999	0.999
E_a (kJ/mol)		3.26			8.02			4.43	
Elovich kinetic model									
α (mg/(g min))	0.237	0.522	0.689	1.115	3.215	7.045	1.129	4.241	24.73
β (g/mg)	0.477	0.349	0.300	0.381	0.372	0.351	0.537	0.515	0.501
R^2	0.988	0.990	0.986	0.978	0.986	0.990	0.991	0.986	0.987
Weber–Morris intraparticle diffusion model									
k_{12} (mg/(g min$^{-1/2}$))	0.261	0.403	0.376	0.277	0.272	0.336	0.249	0.271	0.331
C_2	3.029	4.729	7.917	8.568	10.688	10.760	6.430	8.317	9.454
R^2	0.986	0.980	0.993	0.974	0.991	0.998	0.994	0.997	0.977
Diffusion coefficients									
D_p ($\times 10^{11}$ cm^2/s)	0.947	1.399	1.702	3.712	4.348	4.962	2.673	3.270	3.988
D_f ($\times 10^{11}$ cm^2/s)	0.308	0.686	0.960	1.780	2.405	3.006	1.173	1.694	2.410

3.3.1.2. Freundlich isotherm. In 1906, Freundlich has proposed the earliest known sorption equation. It can be apply to non-ideal adsorption or multilayer sorption of adsorbate on heterogeneous surface based on the following assumptions: (1) the heat of adsorption decrease with increase of surface coverage of adsorbent; (2) the adsorption sites on the surface of adsorbent have different adsorption energies.

At present, Freundlich isotherm is widely used in different heterogeneous systems (Monier, Ayad, Wei, & Sarhan, 2010) and is expressed by the following equation:

$$\ln\ q_e = \ln K_F + \frac{1}{n} \cdot \ln C_e \quad (6)$$

where K_F represents the adsorption capacity for a unit equilibrium concentration, while $1/n$ is the indicative of the energy or intensity of the reaction and suggests the favorability and capacity of the adsorbent–adsorbate system. The values of Freundlich isotherm constants (K_F and $1/n$) determined from the linear plot of $\ln q_e$ versus $\ln C_e$ (Fig. 4a) are presented in Table 3.

Similarly to R_L values from Langmuir isotherm, the $1/n$ value indicates the type of isotherm as follows: irreversible ($1/n = 0$), favorable ($0 < 1/n < 1$), or unfavorable ($1/n > 1$). The Freundlich constants, $1/n$, shown in Table 3 indicate that CF is adsorbed favorably by all the adsorbents used during this study because the values of n are larger than 1.0. The adsorption capacity (K_F) is highest for T_1 microparticles followed by T_2 and A microparticles and is observed that its value increases with the increase of temperature. The values of correlation coefficients (R^2) are higher than Langmuir values. It can be seen that a good fitting of Freundlich model to experimental data is achieved. Similar behavior was observed in adsorption process of acetaminophen, 17α-ethyl estradiol, nalidixic acid, norfloxacin (Lorphensri et al., 2006) and chloramphenicol (Maziad, El-Aal, & El-Kelesh, 2009) on various adsorbents.

Table 5
Kinetic parameters and their correlation coefficients for the adsorption of CF onto A, T_1 and T_2 microparticles (C_{CF} = 700 mg/L).

Sample code	A			T_1			T^2		
T (K)	298	308	313	298	308	313	298	308	313
$q_{e,exp}$ (mg/g)	125.84	148.60	166.82	169.8	179.7	191.19	160.68	175.89	185.30
Lagergren's pseudo first order model									
q_e (mg/g)	118.36	100.64	136.75	11.28	88.42	87.45	84.43	78.20	84.23
k_1 ($\times 10^3$ min^{-1})	8.06	6.06	8.18	6.10	5.27	5.41	6.24	5.71	6.45
R^2	0.943	0.976	0.942	0.930	0.922	0.934	0.952	0.970	0.969
Ho's pseudo-second order model									
q_e (mg/g)	131.23	153.37	171.53	173.31	182.15	193.42	163.13	178.25	187.97
k_2 ($\times 10^4$ g/(mg min))	1.47	1.56	1.62	2.1	2.49	2.56	1.59	1.72	1.83
h (mg/(g min))	2.54	3.68	4.78	6.31	8.28	9.56	4.33	5.61	6.87
R^2	0.999	0.999	0.999	0.998	0.998	0.999	0.999	0.999	0.999
E_a (kJ/mol)		4.95			10.181			7.038	
Elovich kinetic model									
α (mg/(g min))	7.129	15.176	22.489	278.99	3656.51	42719.55	308.46	285.55	409.63
β (g/mg)	0.044	0.042	0.040	0.082	0.072	0.059	0.061	0.054	0.053
R^2	0.980	0.981	0.980	0.976	0.970	0.952	0.989	0.984	0.983
Weber–Morris intraparticle diffusion model									
k_{12} (mg/(g min$^{-1/2}$))	1.576	2.715	3.002	2.304	1.772	1.930	1.849	1.920	2.102
C_2	81.88	78.78	91.01	96.86	118.30	127.90	108.39	124.71	131.51
R^2	0.998	0.998	0.959	0.933	0.977	0.970	0.986	0.987	0.986
Diffusion coefficients									
D_p ($\times 10^{11}$ cm^2/s)	2.170	2.692	3.126	4.543	5.661	6.181	3.133	3.742	4.324
D_f ($\times 10^{11}$ cm^2/s)	0.869	1.273	1.656	2.471	3.258	5.221	1.660	2.160	2.631

Table 6
Kinetic parameters and their correlation coefficients for the adsorption of CF onto A, T_1 and T_2 microparticles (C_{CF} = 3000 mg/L).

Sample code	A			T_1			T_2		
T (K)	298	308	313	298	308	313	298	308	313
$q_{e,exp}$ (mg/g)	413.89	458.47	483.66	566.95	601.40	660.92	498.01	516.00	529.55
The Lagergren's pseudo first order model									
q_e (mg/g)	331.20	366.41	383.66	162.21	150.96	114.34	209.99	191.94	159.15
k_1 ($\times 10^3$ min^{-1})	9.6	9.26	9.37	6.72	6.93	6.52	6.63	6.43	6.17
R^2	0.974	0.949	0.958	0.959	0.960	0.954	0.966	0.956	0.949
The Ho's pseudo-second order model									
q_e (mg/g)	429.18	471.70	495.05	571.43	606.06	662.25	505.05	520.83	534.76
k_2 ($\times 10^5$ g/(mg min))	6.28	6.57	7.15	16.1	18.4	21.4	11.1	12.2	13
h (mg/(g min))	11.56	14.62	17.52	52.44	67.52	94.07	28.34	32.96	37.04
R^2	0.999	0.999	0.999	0.999	0.999	0.999	0.999	0.999	0.999
E_a (kJ/mol)		6.21			14.02			8.02	
Elovich kinetic model									
α (mg/(g min))	32.440	51.158	66.740	6.66x10^3	1.44×10^6	4.39×10^{12}	4.578×10^3	2.11×10^4	8.27×10^7
β (g/mg)	0.014	0.0135	0.0133	0.050	0.029	0.020	0.037	0.025	0.023
R^2	0.974	0.970	0.970	0.980	0.990	0.0992	0.987	0.981	0.983
Weber–Morris intraparticle diffusion model									
k_{12} (mg/(g min$^{-1/2}$))	7.233	4.591	4.750	2.982	2.591	2.922	4.464	4.038	4.353
C_2	249.03	339.16	363.76	487.87	529.29	581.48	378.24	403.54	409.02
R^2	0.923	0.991	0.999	0.998	0.980	0.993	0.989	0.992	0.984
Diffusion coefficients									
D_p ($\times 10^{11}$ cm^2/s)	3.032	3.486	3.982	11.483	13.919	17.690	6.648	7.535	8.244
D_f ($\times 10^{11}$ cm^2/s)	0.982	1.254	1.508	4.536	6.509	9.094	2.678	3.145	3.540

3.3.1.3. Dubinin–Radushkevich isotherm. Another equation used in the analysis of adsorption isotherms was proposed by Dubinin and Radushkevich (Dubinin, Zaverina, & Radushkevich, 1947).

The model was used to estimate the apparent free energy of adsorption as well as to make a difference between physical and chemical adsorption process. The D–R equation was given by the following relationship:

$$\ln\ q_e = \ln q_m - \beta\varepsilon^2 \tag{7}$$

where q_m is the theoretical saturation capacity, β is the activity coefficient related to mean sorption energy and ε is the Polanyi potential given by:

$$\varepsilon = RT\ \ln\left(1 + \frac{1}{C_e}\right) \tag{8}$$

where R is the gas constant (8.314 kJ/(mol K)) and T is the temperature (K).

The values of isotherm constants (q_m and β) obtained by plotting $\ln q_e$ versus ε^2 (figure not shown) are given in Table 3. The constant q_m agreed well with experimental data. The D–R constant β can give the valuable information regarding the mean energy of adsorption by the following equation:

$$E = \frac{1}{\sqrt{-2\beta}} \tag{9}$$

It is known that the magnitude of E gives the information about the type of adsorption process: physical (1-8 kJ/mol), ion exchange (9–16 kJ/mol) and chemical (>16 kJ/mol) (Chabani, Amrane, & Bensmaili, 2006). The apparent free energies of CF adsorption on A, T_1 and T_2 microparticles were calculated to be in the range

Table 7
Kinetic parameters and their correlation coefficients for the adsorption of CF onto A, T_1 and T_2 microparticles (C_{CF} = 3750 mg/L).

Sample code	A			T_1			T_2		
T (K)	298	308	313	298	308	313	298	308	313
$q_{e,exp}$ (mg/g)	458.23	579.3	614.84	618.2	698.4	783.62	567.42	674.3	720.83
The Lagergren's pseudo first order model									
q_e (mg/g)	298.11	318.13	238.99	160.48	118.24	98.52	173.34	188.53	139.75
k_1 ($\times 10^3$ min^{-1})	7.85	7.62	6.08	6.82	5.53	5.46	4.65	5.59	4.12
R^2	0.961	0.972	0.978	0.996	0.978	0.989	0.982	0.975	0.980
The pseudo-second order model									
q_e (mg/g)	469.48	588.24	625	621.12	699.30	787.40	574.71	680.27	724.64
k_2 ($\times 10^5$ g/(mg min))	7.49	7.99	8.87	17.9	18.7	24.8	10.1	11.1	12.1
h (mg/(g min))	16.51	27.65	34.65	69.06	91.58	153.85	33.36	50.79	63.57
R^2	0.999	0.999	0.999	0.999	0.999	0.999	0.999	0.999	0.999
E_a (kJ/mol)		8.16			14.78			9.01	
Elovich kinetic model									
α (mg/(g min))	91.11	277.23	926.73	2.28×10^5	1.52×10^{12}	3.35×10^{13}	6.99×10^4	1.06×10^5	3.19×10^8
β (g/mg)	0.0131	0.0127	0.0121	0.046	0.044	0.025	0.032	0.026	0.022
R^2	0.967	0.970	0.975	0.967	0.992	0.982	0.987	0.973	0.989
Weber–Morris intraparticle diffusion model									
k_{12} (mg/(g min$^{-1/2}$))	4.688	5.645	6.484	4.542	3.160	2.444	6.629	5.517	4.603
C_2	332.47	436.85	455.39	510.65	610.72	717.81	397.48	529.45	591.04
R^2	0.991	0.984	0.991	0.967	0.989	0.993	0.993	0.941	0.987
Diffusion coefficients									
D_p ($\times 10^{11}$ cm^2/s)	3.956	5.288	6.237	13.876	16.323	24.373	6.883	8.954	10.403
D_f ($\times 10^{11}$ cm^2/s)	1.009	1.702	2.195	4.791	6.361	10.800	2.306	3.565	4.427

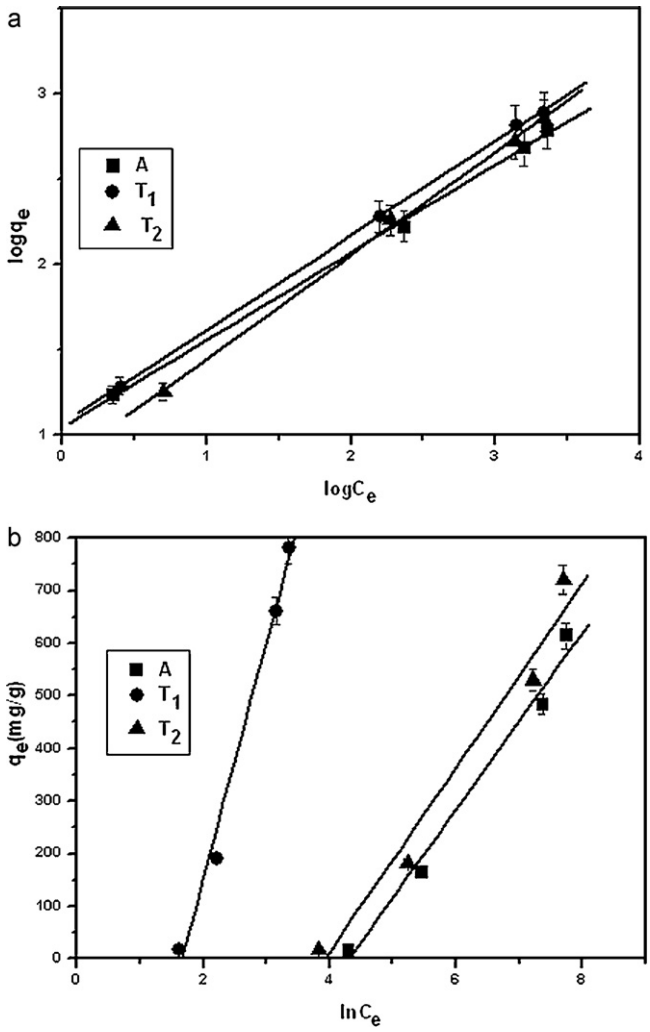

Fig. 4. Equilibrium adsorption isotherms of CF on A, T_1 and T_2 microparticles at 313 K fitted to: Freundlich model (a) and Temkin model (b).

of 2.59–7.94 kJ/mol, which means that the process is physical adsorption.

3.3.1.4. Temkin isotherm. Temkin and Pyzhev isotherm was proposed to describe for the first time the adsorption of hydrogen onto platinum electrodes within the acidic solution (Temkin & Pyzhev, 1940). The assumptions made on the Temkin adsorption model are that: (a) adsorption is characterized by a uniform distribution of binding energies; (b) the heat of adsorption of all the molecules in the layer would decrease linearly with coverage due to adsorbent–adsorbate interactions.

The linear form of Temkin isotherm was given below:

$$q_e = B \cdot \ln\ a_T + B \cdot \ln C_e \tag{10}$$

$$B = \frac{RT}{b_T}$$

where b_T is the Temkin constant related to the heat of adsorption (J/mol) and a_T is the equilibrium binding constant corresponding to the maximum binding energy (L/mg).

By plotting q_e against $\ln C_e$ (Fig. 4b) it can be obtained the Temkin constants a_T and b_T as intercept and slope. The values of the Temkin parameters are given in Table 3. Based on correlation coefficient shown in Table 3 the results indicate that the Freundlich and Dubinin–Radushkevich models represent a better fit of experimental data than Langmuir and Temkin models.

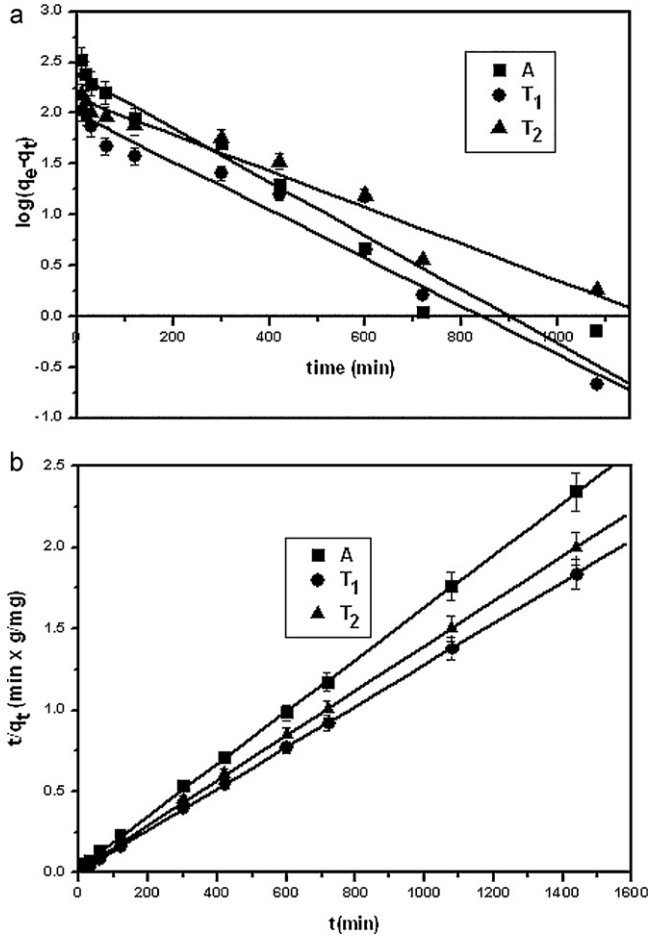

Fig. 5. Pseudo first-order kinetics (a) and pseudo second-order kinetics (b) for adsorption of CF on A, T_1 and T_2 microparticles at 313 K and C_{CF} = 3750 mg/L.

3.3.2. Kinetic studies

Several models can be used to express the mechanism of solute adsorption onto an adsorbent. In this study the experimental data were interpreted by: pseudo-first-order, pseudo-second-order, intraparticle diffusion and Elovich models.

3.3.2.1. The pseudo-first order equation. In 1898, Lagergren was developed a conventional method used to describe the adsorption of an adsorbate from the liquid phase on a solid phase (Lagergren, 1898). The linear form of pseudo-first-order equation is given as:

$$\log(q_e - q_t) = \log\ q_e - \frac{k_1}{2.303} \cdot t \tag{11}$$

where k_1 is the rate constant of the pseudo-first order adsorption process (min^{-1}).

The straight line plot of log $(q_e - q_t)$ against t (Fig. 5a) gave the slope of k_1 and intercept of $q_{e(calc)}$.

The calculated k_1 values and their corresponding linear correlation coefficient values are shown in Tables 4–7.

From Tables 4–7 it can be observed that the experimental $q_{e(exp)}$ values did not agree with the theoretical values calculated $q_{e(calc)}$ from Eq. (11). Moreover, the correlation coefficient for the Lagergren model obtained at all the studied concentrations and temperatures were in the range 0.922–0.988, indicating that the first order model does not reproduce the adsorption kinetics of CF on A, T_1 and T_2 microparticles.

3.3.2.2. The pseudo-second order kinetic model. Ho and McKay (1998) have proposed a second order kinetic model based on equilibrium adsorption. The pseudo-second order equation is expressed as:

$$\frac{t}{q_t} = \frac{1}{h} + \frac{1}{q_e} \cdot t \tag{12}$$

$$h = k_2 \cdot q_e^2$$

where h is the initial sorption rate and k_2 is the rate constant of pseudo-second order adsorption (g/mg min). The slopes and intercepts of plots t/q_t versus t were used to calculate the q_e and h (Fig. 5b).

The adsorption rate constant (k_2), adsorption capacity (q_e) and correlation coefficient values for the CF adsorption on A, T_1 and T_2 microparticles are presented in Tables 4–7. From Tables 4–7 one can see that in case of pseudo-second order the theoretical $q_{e(calc)}$ values agree well with the experimental uptake values, $q_{e(exp)}$ and the correlation coefficients are close to 1.0 for all three samples. Also, this model is more likely to predict the behavior over the whole experimental range of adsorption than pseudo-first order model. Moreover, it can be observed that for the same kind of adsorbent the values of k_2 increase with increasing temperature, indicating a higher diffusion rate of drug molecule at higher temperatures.

3.3.2.3. Weber and Morris intraparticle diffusion model. The adsorbate molecules can be transferred from the solution phase over an adsorbent in three consecutive steps (Sarici-Ozdemir & Onal, 2010):

(a) transport of the adsorbate ions to the external surface of adsorbent (film diffusion);
(b) transport of the adsorbate molecules within the pores of adsorbent (intraparticle diffusion);
(c) adsorption of the adsorbate molecules on the interior surface of the adsorbent.

The possibility of intraparticle diffusion was explored by Weber and Morris using the following expression:

$$q_t = K_{id} \cdot t^{1/2} + C_i \tag{13}$$

where K_{id} is the intraparticle diffusion rate constant (g/mg min$^{1/2}$) and C_i is the constant that gives an idea about the thickness of the boundary layer. The higher values of C_i depict higher adsorption capacity.

The straight line plots of q_t against $t^{1/2}$ were used to determine the intraparticle diffusion rate (K_{id}) and correlation coefficient. For example, in Fig. 6 is shown the representation of the intraparticle diffusion model for A, T_1 and T_2 microparticles at 313 K and drug solution concentration of 3750 mg/L.

According to the Eq. (13), if the plot gives a straight line, then the adsorption is controlled solely by the intraparticle diffusion, but of the adsorption data present a multi-linear plot it shows that there are two or more steps involving in the adsorption process (Srivastava, Swamy, Mall, Prasad, & Mishra, 2006).

As can be seen from Fig. 6, the adsorption was controlled by three different stages: (1) rapid external surface adsorption or instantaneous adsorption stage; (2) gradual adsorption where intraparticle diffusion is rate-controlled and (3) final equilibrium stage due to the low concentration of CF in solution phase, as well as to the less number of available adsorption sites.

The values of the diffusion rate constant C_i and the correlation coefficient are given in Tables 4–7. It was observed that the values of C_i increased with the initial concentration of drug, which indicates an increase in thickness and the effect of the boundary layer. However, the intercept of the line fails to pass through the origin

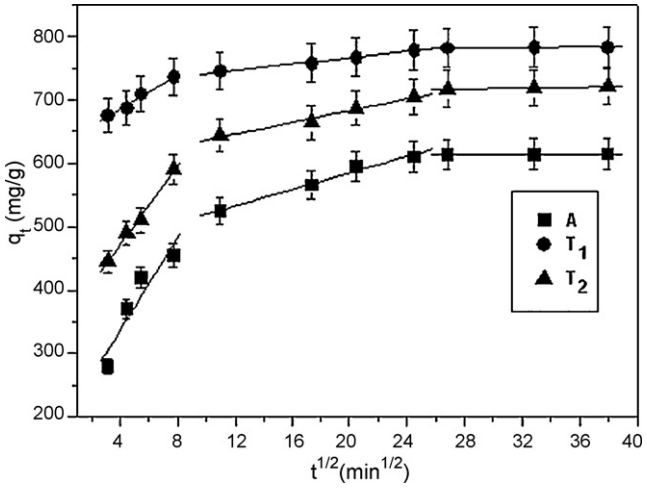

Fig. 6. Plot of Weber–Morris intraparticle diffusion model for CF adsorption on A, T_1 and T_2 microparticles at 313 K and C_{CF} = 3750 mg/L.

which may be due to the difference in the rate of mass transfer in the initial and final stages of adsorption.

Based on these results it might be concluded that the intraparticle diffusion was not the only rate-limiting step. Therefore, the adsorption process may be a complex nature consisting of both surface adsorption and intraparticle diffusion. Furthermore, all of these suggest that the adsorption of CF on A, T_1 and T_2 microparticles might be controlled by external mass transfer followed by intraparticle diffusion.

3.3.2.4. Diffusion coefficients. The film diffusion (D_f, cm^2/s) and diffusion within the adsorbent (pore diffusion, D_p, cm^2/s) control the intraparticle diffusion process.

Assuming that the solid phase consists of spherical particles the film and pore diffusion coefficients can be expressed by:

$$D_p = 0.03 \cdot \frac{R_p^2}{t_{1/2}} \ (\text{cm}^2/\text{s}) \tag{14}$$

$$D_f = 0.23 \cdot \frac{R_p \cdot \varepsilon}{t_{1/2}} \cdot \frac{q}{C_0} \ (\text{cm}^2/\text{s}) \tag{15}$$

where R_p is the radius of the adsorbent which was calculated as the average radius between the radii corresponding the highest and lower size fractions [R_p (A) = 184 μm, R_p (T_1) = 189 μm, R_p (T_2) = 187 μm], ε is the film thickness (10^{-3} cm) (Chabani et al., 2006), q is the amount of CF adsorbed (mg/L) and $t_{1/2}$ is the half-adsorption time.

The half adsorption time, $t_{1/2}$, is a parameter which can be calculated by using the following equation (Dogan, Ozdemir, & Alkan, 2007):

$$t_{1/2} = \frac{1}{k_2 \cdot q_e} \tag{16}$$

The values of the film and pore diffusion coefficient at different concentrations and temperatures are presented in Tables 4–7. D_p and D_f values are in the range 0.308×10^{-11}–$24.373\,10^{-11}$ cm^2/s and the values increase with the increase of temperature and concentration of CF.

3.3.2.5. Elovich equation. Eq. (17), known as Elovich equation has been first proposed in 1934 by Roginsky and Zeldovich and is extensively applied to biosorption data (Hameed, Tan, & Ahmad, 2008). The general mathematical expression is:

$$q_t = \frac{1}{\beta} \cdot \ln(\alpha \cdot \beta) + \frac{1}{\beta} \cdot \ln\ t \tag{17}$$

Table 8
Thermodynamic parameters.

Sample code	Temperature (*K*)	$-\Delta G$ (kJ/mol)	ΔH (J/mol)	ΔS (J/(mol K))	R^2
A	298	10.104	9.467	65.675	0.991
	308	10.761			
	313	11.089			
T_1	298	11.272	17.395	96.198	0.999
	308	12.234			
	313	12.715			
T_2	298	10.446	16.858	91.624	0.995
	308	11.362			
	313	11.820			

where α is the initial adsorption rate (mg/(g min)) and β is the desorption constant (g/mg). Both kinetic constants (α and β) will be estimated from the slope and intercept of the plot q_t versus $\ln t$ (figure not shown).

The kinetic constants obtained from the Elovich equation and the correlation coefficients are presented in Tables 4–7. The R^2 values between 0.952 and 0.992 indicate that the experimental data do not fit well the Elovich kinetic model.

3.4. Estimation of thermodynamic parameters

3.4.1. Gibbs free energy changes

In order to describe the effect of temperature and the feasibility of the adsorption process of CF onto A, T_1 and T_2 microparticles, thermodynamic parameters such as Gibbs free energy changes (ΔG), enthalpy change (ΔH) and entropy change (ΔS) were also calculated. The experiments were carried out at temperatures of 298, 308 and 313 K. By means of the Langmuir equilibrium constant (K_L) (Table 3), the enthalpy and entropy change values of CF adsorption can be estimated using the van t'Hoff equation (Rodriguez, Garcia, Ovejero, & Mestanza, 2009):

$$\ln K_L = \frac{\Delta S}{R} - \frac{\Delta H}{RT} \tag{18}$$

According to Eq. (18) the ΔH and ΔS values were calculated from the slope and intercept of linear regression of $\ln K_L$ against $1/T$ (Fig. 7). Then, with a well-known equation the ΔH and ΔS values were used to calculated ΔG value:

$$\Delta G = \Delta H - T \cdot \Delta S \tag{19}$$

The thermodynamic parameters are given in Table 8. As seen from Table 8 adsorption enthalpy values are relatively low ($\Delta H < 40$ kJ/mol), indicating that the interactions between microparticles and drug molecules are physical (Wang Ngah & Hanafiah, 2008). On the other hand the positive value of adsorption enthalpy shows that the adsorption process is endothermic, this behavior of ΔH indicating that higher temperature led to the increase of the CF amount adsorbed.

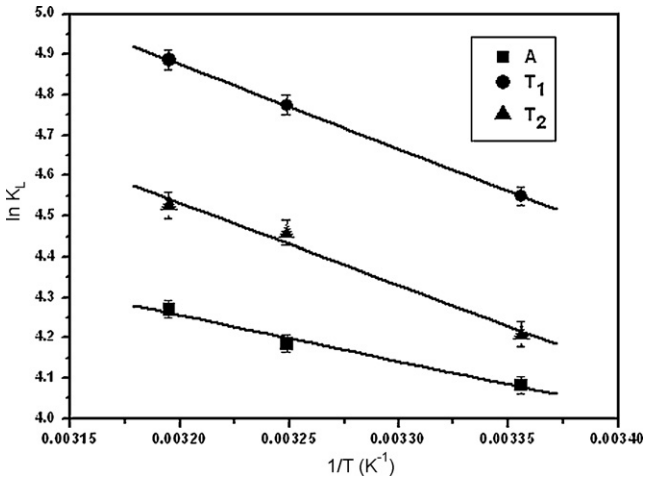

Fig. 7. Plot of $\ln K_L$ versus $1/T$ for the estimation of thermodynamic parameters for adsorption of CF on A, T_1 and T_2 microparticles.

The positive value of ΔS reflects the affinity of A, T_1 and T_2 microparticles for CF and suggests some structural changes in adsorbate and adsorbent. In addition, the positive ΔS values indicate an irregular increase of the randomness at the microparticles–solution interface during CF adsorption (Thinakaran, Baskaralingam, Ravi, Panneerselvam, & Sivanesan, 2008).

The ΔG is a fundamental criterion to determine if a process occurs spontaneously. The negative values of ΔG indicate the feasibility of the process and the spontaneous nature of the adsorption process. From Table 8 it can observe that the ΔG values are more than −20 kJ/mol and less than 0. It should be mentioned that, the values of ΔG are in the range of multilayer adsorption which occurs by both physical adsorption and weak chemical interaction. These results are confirmed by those obtained from the adsorption isotherms when Freundlich isotherm has been fitted for the adsorption of CF on microparticles. The decrease of ΔG value with an increase of temperature indicates that the adsorption process of CF on microparticles becomes more favorable at higher temperature.

3.4.2. Activation energy

The magnitude of the activation energy (E_a) may give information about the type of adsorption process which can be physical or chemical. The physisorption process has a low activation energy values (5–40 kJ/mol) while the chemisorption has a higher activation energy values (40–800 kJ/mol) (Wu, 2007). These values of E_a indicate that the physisorption is a diffusion controlled process while the chemisorption is chemically controlled process.

The activation energy of CF adsorption was calculated from the linear form of Arrhenius equation (Hasan, Ahmad, & Hameed, 2008):

$$\ln k_2 = \ln A - \frac{E_a}{RT} \tag{20}$$

where k_2 is the pseudo-second order rate constant (g/mg min), A is Arrhenius factor and E_a is the Arrhenius activation energy (kJ/mol).

The E_a values were determined from the slope of $\ln k_2$ versus $1/T$ (figure not shown).

The values of activation energy (3.26–14.78 kJ/mol) presented in Tables 4–7 confirm the nature of physisorption process of CF onto A, T_1 and T_2 microparticles. The positive value of E_a suggested that rise in temperature favor the CF adsorption and this process may be an endothermic in nature.

4. Conclusions

In the present work, the adsorption capacities of the ion exchange resin and polymer coated ion exchange resin micropar-

ticles were reported. Some conclusions may be drawn as follows:

- Drug adsorption capacity of T microparticles is considerably higher than that for A microparticles.
- Equilibrium adsorption of CF by A and T microparticles was analyzed by the Langmuir, Freundlich, Temkin and Dubinin–Radushkevich models and indicate that the Freundlich and Dubinin–Radushkevich models represent a better fit of experimental data.
- The adsorption energy obtained by Dubinin–Radushkevich isotherm suggested the physisorption nature of the adsorption process.
- Analysis of the kinetic and rate data, at different conditions (temperature and drug concentrations) using the pseudo-first order, pseudo-second order, intraparticle diffusion, Elovich models revealed that the pseudo second-order sorption mechanism is predominant and the correlation coefficients are higher than 0.998.
- Thermodynamic constants were evaluated using the Langmuir constants, K_L, at different temperatures. The positive values of ΔH and ΔS and negative values of ΔG showed the endothermic and the spontaneous nature of the adsorption process.

Acknowledgement

This study was supported by grant from the Ministry of Education and Research of Romania.

References

Abdekhodaie, M. J., & Wu, X. Y. (2006). Drug loading onto ion-exchange microspheres: Modeling study and experimental verification. *Biomaterials*, *27*, 3652–3662.

Albertini, B., Passerini, M., Gonzalez-Rodriguez, M. L., Cavallari, C., Crini, M., & Rodriguez, L. (2008). Wet granulation as innovative and fast method to prepare controlled release granules based on an ion-exchange resin. *Journal of Pharmaceutical Science*, *97*, 1313–1324.

Angelin, B., & Einarsson, K. (1981). Cholestyramine in type IIa hyperlipoproteinemia: Is low-dose treatment feasible? *Atherosclerosis*, *38*, 33–38.

Atyabi, F., Sharma, H. L., Mohammad, H. A. H., & Fell, J. T. (1996). In vivo evaluation of a novel gastric retentive formulation based on ion exchange resins. *Journal of Controlled Release*, *42*, 105–113.

Belakhov, V. V., & Momot, N. N. (1983). Regeneration of FAF and AV-17I anion exchange resins after absorption purification of α-amylase from *Bacillus subtilis*. *Pharmaceutical Chemistry Journal*, *17*, 369–371.

Bunia, I., Neagu, V., & Luca, C. (2006). Chemical transformation of different acrylic crosslinked polymers with primary amines and some applications of the synthesized compounds. *Reactive and Functional Polymers*, *66*, 871–883.

Chabani, M., Amrane, A., & Bensmaili, A. (2006). Kinetic modelling of the adsorption of nitrates by ion exchange resin. *Chemical Engineering Journal*, *125*, 111–117.

Chen, A. H., & Huang, Y. Y. (2010). Adsorption of Remazol Black 5 from aqueous solution by the templated crosslinked-chitosans. *Journal of Hazardous Materials*, *177*, 668–675.

Ciardelli, G., Chiono, V., Vozzi, G., Pracella, M., Ahluwalia, A., Barbani, N., et al. (2005). Blends of poly(ε-caprolactone) and polysaccharides in tissue engineering applications. *Biomacromolecules*, *6*, 1961–1976.

Conaghey, O. M., Corish, J., & Corrigan, O. I. (1998). The release of nicotine from a hydrogel containing ion exchange resins. *International Journal of Pharmaceutics*, *170*, 215–221.

Connors, K. A., Amidon, G. L., & Stella, V. J. (1986). *Chemical stability of pharmaceutics: Handbook for pharmacists.* (2nd ed.). New York: John Wiley and Sons., pp. 302–308.

Dogan, M., Ozdemir, Y., & Alkan, M. (2007). Adsorption kinetics and mechanism of cationic methyl violet and methylene blue dyes onto septiolite. *Dye and Pigments*, *75*, 701–713.

Dubinin, M. M., Zaverina, E. D., & Radushkevich, L. V. (1947). Sorption and structure of active carbons. I. Adsorption of organic vapors. *Zhurnal Fizicheskoi Khimii*, *21*, 1351–1362.

Dulman, V., Simion, C., Barsanescu, A., Bunia, I., & Neagu, V. (2009). Adsorption of anionic textile dye Acid Green 9 from aqueous solution onto weak or strong base anion exchangers. *Journal of Applied Polymer Science*, *113*, 615–627.

Fundueanu, G., Constantin, M., Esposito, E., Cortesi, R., Nastruzzi, C., & Menegatti, E. (2005). Cellulose acetate butyrate microcapsules containing dextran ion exchange resin as self-propelled drug release system. *Biomaterials*, *26*, 4337–4347.

Hameed, B. H., Tan, I. A. W., & Ahmad, A. L. (2008). Adsorption isotherm, kinetic modeling and mechanism of 2,4,6-trichlorophenol on coconut husk-based activated carbon. *Chemical Engineering Journal*, *144*, 235–244.

Hasan, M., Ahmad, A. L., & Hameed, B. H. (2008). Adsorption of reactive dye onto crosslinked chitosan/oil palm ash composite beads. *Chemical Engineering Journal*, *136*, 164–172.

Ho, Y. S., & McKay, G. (1998). The kinetics of sorption of basic dyes from aqueous solution by Sphagnum moss peat. *The Canadian Journal of Chemical Engineering*, *76*, 822–827.

Holmberg, A. R., Wilchek, M., Marquez, M., Westlin, J. E., Du, J., & Nilsson, S. (1999). Ion exchange tumor targeting: A new approach. *Clinical Cancer Research*, *5*, 3056s–3058s.

Jeong, S. H., Berhane, N. H., Haghighi, K., & Park, K. (2007). Drug release properties of polymer coated ion-exchange resin complexes: Experimental and theoretical evaluation. *Journal of Pharmaceutical Sciences*, *96*, 618–632.

Lagergren, S. (1898). About the theory of so-called adsorption of soluble substances. *Kungliga Svenska Vetenskapsakademiens Handlingar Band*, *24*, 1–39.

Lorphensri, O., Intravijit, J., Sabatini, D. A., Kibbey, T. C. G., Osathaphan, K., & Saiwan, C. (2006). Sorption of acetaminophen 17α-ethynyl estradiol, nalidixic acid and norfloxacin to silica, alumina and a hydrophobic medium. *Water Research*, *40*, 1481–1491.

Maziad, N. A., El-Aal, S. E. A., & El-Kelesh, N. A. (2009). Equilibrium adsorption isotherm and controlled release of antibiotic drug chloramphenicol from poly(2-vinylpyridine/acrylic acid) hydrogels prepared by gamma radiation. *Journal of Applied Polymer Science*, *111*, 1369–1380.

Monier, M., Ayad, D. M., Wei, Y., & Sarhan, A. A. (2010). Adsorption of Cu(II), Co(II) and Ni(II) ions by modified magnetite chitosan chelating resin. *Journal of Hazardous Materials*, *177*, 962–970.

Neagu, V., Untea, I., Tudorache, E., & Orbeci, C. (2004). Sorption equilibrium of Cr(VI) ions by strong base anion exchangers with pyridine structures. *Journal of Applied Polymer Science*, *93*, 1957–1963.

Rodriguez, A., Garcia, J., Ovejero, G., & Mestanza, M. (2009). Adsorption of anionic and cationic dyes on activated carbon from aqueous solutions: Equilibrium and kinetics. *Journal of Hazardous Materials*, *172*, 1311–1320.

Sand, A., Yadav, M., & Behari, K. (2010). Graft copolymerization of 2-acrylamidoglycolic acid on to xanthan gum and study of its physicochemical properties. *Carbohydrate Polymers*, *81*, 626–632.

Sarici-Ozdemir, C., & Onal, Y. (2010). Equilibrium, kinetic and thermodynamic adsorptions of the environmental pollutant tannic acid onto activated carbon. *Desalination*, *251*, 146–152.

Srivastava, Y. C., Swamy, M. M., Mall, I. D., Prasad, B., & Mishra, I. M. (2006). Adsorptive removal of phenol by bagasse fly ash and activated carbon: Equilibrium, kinetics and thermodynamics. *Colloid and Surfaces A: Physicochemical and Engineering Aspects*, *272*, 89–104.

Sterns, R. H., Rojas, M., Bernstein, P., & Chennupati, S. (2010). Ion exchange resins for treatment of hyperkalemia: Are they safe and effective? *Journal of the American Society of Nephrology*, *21*, 733–735.

Temkin, M. I., & Pyzhev, V. (1940). Kinetics of ammonia synthesis on promoted iron catalyst. *Acta Physico Chemica USSR*, *12*, 327–356.

Thinakaran, N., Baskaralingam, P., Ravi, K. V. T., Panneerselvam, P., & Sivanesan, S. (2008). Adsorptive removal of Acid Blue 15: Equilibrium and kinetic study. *Clean-Soil, Air, Water*, *36*, 798–804.

Wang Ngah, W. S., & Hanafiah, M. A. K. M. (2008). Adsorption of cooper on rubber (*Hevea brasiliensis*) leaf powder: Kinetic, equilibrium and thermodynamic studies. *Biochemical Engineering Journal*, *39*, 521–530.

Wawrzkiewicz, M., & Hubicki, Z. (2010). Equilibrium and kinetic studies on the sorption of acidic dye by macroporous anion exchanger. *Chemical Engineering Journal*, *157*, 29–34.

Weber, T. W., & Chakravot, R. K. (1974). Pore and solid diffusion models for fixed bed adsorbents. *AiChE Journal*, *20*, 228–238.

Wrong, O., & Harland, C. (2007). Sevelamer and other anion-echange resins in the prevention and treatment of hyperphosphatemia in chrionic renal failure. *Nephron Physiology*, *107*, 17–33.

Wu, C. H. (2007). Adsorption of reactive dye into carbon nanotubes: Equilibrium, kinetics and thermodynamics. *Journal of Hazardous Materials*, *144*, 93–100.